Energy Conversion and Management: X 24 (2024) 100769

Contents lists available at ScienceDirect

Energy Conversion and Management: X

journal homepage: www.sciencedirect.com/journal/energy-conversion-and-management-x

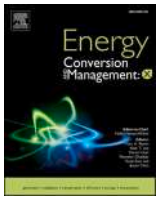

Energy and exergy assessment of a photovoltaic-thermal (PVT) system cooled by single and hybrid nanofluids

Mohammed Alktranee [a], Qudama Al-Yasiri [b], Karrar Saeed Mohammed [c], Hayder Al-Lami [b], Péter Bencs [d,*]

[a] Department of Mechanical Techniques, Technical Institute of Basra, Southern Technical University, Basrah, Iraq
[b] College of Engineering, University of Misan, Al Amarah City, Maysan, 62001, Iraq
[c] Department of Medical Physics, Al-Manara College for Medical Sciences, Maysan, Iraq
[d] Department of Fluid and Heat Engineering, Faculty of Mechanical Engineering and Informatics, University of Miskolc, Miskolc, HU-3515, Hungary

ARTICLE INFO

Keywords:
PVT
Exergy efficiency
Energy efficiency
Nanofluid
Nusselt number

ABSTRACT

Photovoltaic-thermal (PVT) concept is a novel methodology to lower the PV module temperature and consecutively produce thermal and electrical energies. This study assesses the thermal and electrical advancements of a PVT system using iron oxide (Fe_2O_3) single nanofluid and titanium oxide-iron oxide (TiO_2-Fe_2O_3) hybrid nanofluid at 0.2 % and 0.3 % concentrations. The PVT energy and exergy efficiencies were presented and analyzed concerning the effect of proposed single and hybrid nanofluids. Study findings disclosed that dispersing 0.3% of TiO_2- Fe_2O_3 nanocomposites into water has enhanced the nanofluid thermal conductivity, improving the Nusselt number by 90.64 %, while Fe_2O_3 nanoparticles achieved 31.75 %. Furthermore, employing TiO_2- Fe_2O_3-based nanofluid at 0.3 % has enhanced the PVT electrical efficiency by 13 % and, thermal efficiency by 44 % compared to Fe_2O_3-based nanofluid, which exhibited 12 %, and 33 %, respectively. Besides, the PVT electrical exergy efficiency was augmented by about 13 % using TiO_2-Fe_2O_3-based hybrid nanofluid, against 11 % using Fe_2O_3 nanofluid. Reversely, the pressure drop was increased by a maximum of 62.9% when TiO_2- Fe_2O_3 was applied due to the raised nanofluid density compared to the reference base fluid. Conclusively, hybrid nanofluid has a superior influence on the PVT performance than single nanofluids. However, further investigations are required to explore cost-effective hybrid nanofluids with a low pressure drop.

1. Introduction

The energy sector encounters a great challenge year after year due to the increase in humankind's energy requirements and the danger of climate change. Besides, global economic growth in modern society is contingent upon the availability of energy although numerous concerns arise in the energy sector, such as scarcity of energy resources and escalating energy needs for human measures [1]. Nowadays, fossil fuels are the primary electric power foundation which contributes to air pollutants and greenhouse gases. Alongside the volatility of fossil fuel costs, other concerns have encouraged the adoption of renewable energies in various energy sectors, especially solar-based ones [2]. Solar energy is leading the widespread solutions proposed in this regard due to its sustainability, reliability, cost-effectiveness, environmentally-friendly and flexibility to be used in different applications [3]. Solar systems are highly efficient renewable energy methods to harness sunlight and generate thermal or electrical energies. In the electric generation field, photovoltaic (PV) technology is a fundamental solar system to produce electricity, occupying a wide range of industrial, agricultural, and domestic applications [4–6]. However, the main weakness of this technology is the rising operating temperature due to the low conversion efficiency of PV modules especially in hot regions [7]. Since PV modules are generally made from semiconductors, increased solar radiation and ambient temperature heating the module, cause degradation in the conversion efficiency, particularly when the operation temperature exceeds 25 °C [8,9]. Besides, it was reported that increasing the PV module temperature by more than 45 °C causes a degradation in the conversion efficiency, and local hotspots may appear, which reduces its lifetime [10]. Therefore, energy production from PV modules needs to be adjusted towards optimal operation conditions by maintaining the operating temperatures at an optimal level. Various passive and active techniques were introduced in the literature to minimize the PV cell temperature and improve its overall efficiency.

* Corresponding author.
E-mail address: peter.bencs@uni-miskolc.hu (P. Bencs).

https://doi.org/10.1016/j.ecmx.2024.100769
Received 22 August 2024; Received in revised form 3 October 2024; Accepted 20 October 2024
Available online 22 October 2024

Nomenclature

A	PV module area, m^2
C_p	Specific heat, kJ/kg. °C
S	Solar radiation, W/m^2
I_{SC}	Short circuit current, A
I_{pv}	Electric current, A
K	Thermal conductivity, W/m·K
$\dot{m}$	mass flow rate, L/min
P_{pv}	Electrical power, W
T	Temperature, °C
TiO_2	Titanium oxide
V_{pv}	Voltage, V
Nu	Nusselt number
T_{avg}	Average temperature °C
Re	Reynolds number
Pr	Prandt Number

Subscript

amb	Ambient
DI	Deionized
FF	Fill factor
bf	Base fluid
in	Input
np	Nanoparticles
out	Output
nf	nanofluid
g	Gravity, m/s^2
D_t	Tube diameter, m
PV	Photovoltaic

Greek symbols

η_{th}	Thermal efficiency, %
η_{ov}	Overall efficiency, %
η_{el}	Electrical efficiency, %
ρ	Density, kg/m^3
μ	Viscosity, kg/ms
$\dot{E}x$	Exergy, W
$\eta_{\dot{E}_x}$	Exergy efficiency, %
φ	Volume concentration, %
NWs	Nanowires

Passive methods mainly involved the use of fins [11], turbulators [12], phase change materials [13], thermoelectric generators [14], radiative cooling coatings [15], tracking mechanisms [16] and many others. Besides, active techniques included the use of air flow [17], water stream [18], bi-fluids [19], geothermal energy [20], and nanofluids [21]. However, several studies considered emerging methods by integrating two or more passive/ active techniques [22–26].

The photovoltaic-thermal (PVT) approach is one of the advanced solutions, which includes a PV module and a heat exchanger (collector) with an absorbent plate and attached tubes or channels to the rear of the PV module [27]. Researchers have mainly considered two paths in the PVT technology; enhancing the heat exchanger geometry using micro channels heat sinks, internal and external extended surfaces, and/or applying novel nanofluids [28–30]. In the latter technique, cooling fluids are circulated on the rear side of the PV module to help reduce its temperature and reuse the absorbed heat in other thermal applications, which improves the system efficiency [31]. Water is commonly employed as a cooling fluid in PVT systems although it showed limited improvements in the system performance due to its relatively low thermal conductivity [32]. Therefore, nano-based fluids were introduced as an appropriate coolant due to their high thermal properties compared to water [33]. Nano-based systems are revolutionary technology nowadays which involved in many thermal applications, including buildings, transportation, power generation and other traditional and renewable energy sectors [34–38].

Several attempts have been carried out by researchers to improve the PVT thermal performance by employing single nanofluids [39,40]. For instance, Chen et al. [41] numerically investigated the potential of the aluminium oxide (Al_2O_3)-based nanofluid to cool a standard PVT system. An empirical formula was developed to predict the PVT temperature reduction and efficiency at various concentrations and mass flow rates. Outcomes indicated that the PVT average temperature was reduced by a maximum of 8.92 ℃ at 5 % concentration. Besides, the temperature decrement was further increased to 9.94 ℃, when increasing the nanofluid mass flow rate to 0.12 m^3/h. however, the PVT efficiency was predicted to increase from 10.84 % to 12.36 % when increasing the Al_2O_3/water from 1 % to 5 %, compared to a standard PV module. Venkatesh et al. [42] experimentally examined the thermal contribution of graphene nanoplatelets (GnPs)/water nanofluid to a PVT efficiency under 0.085, 0.075, and 0.065 kg/s mass flow rates, and 0 %-0.3 % concentrations. The study outcomes demonstrated that incorporating GnPs/water nanofluids has reduced the PVT surface temperature by a maximum of 20 °C at 0.3 % concentration and 0.085 kg/s flow rate. Correspondingly, GnPs/water nanofluid has improved the PVT energy efficiency by about 23 %. Menon et al. [43] experimentally explored the influence of CuO/water nanofluid in a serpentine tube integrated unglazed PVT system to advance building performance and increase efficiency. Study results showed that water cooling has reduced the PVT temperature by 15 °C and enhanced electrical efficiency by about 12.32 % more than the reference PV module, which attained 12.98 %. Besides, employing CuO/water nanofluid has incremented the electrical efficiency by 35.67 % as a result of reducing the PV module's temperature by about 23.7 °C. The research concluded that the dispersing of CuO nanoparticles into water has improved its thermal conductivity drastically. In this way, the thermal efficiency in the case of CuO nanoparticles dispersion was exceeded up to 71.17 % compared with water which conversely delivered a peak thermal efficiency of 58.77 %. Another indoor experiment was conducted by Nasrin et al. [44] on a PVT system under 200–1000 W/m^2 solar radiation, 32 °C inlet temperature, and 0.5 L/min of constant mass flow rate. The system was cooled by MWCNT nanofluid with different concentrations, ranging from 0 % to 1 % circulated into aluminium pipes, connected to the backside of the PVT system. Moreover, numerical simulations were carried out for the PVT system 3D module under the same operation conditions using COMSOL Multiphysics software. The numerical outcomes displayed good agreement with the experimental results in which the PVT system efficiency was enhanced by 9.2 % when cooled by water. Moreover, system thermal performance was improved numerically by 4 % and experimentally by 3.67 % when cooling by nanofluid. The maximum numerical overall efficiency calculated was 89.2 %, against 87.65 % in the experimentation under the nanofluid cooling and 1000 W/m^2 solar irradiation. Hissouf et al. [45] proposed Cu and Al_2O_3 nanofluids for cooling a PVT system by building a mathematical model derived from energy balance equations of system components. The research outcomes showed that the PVT electrical and thermal efficiencies were enhanced by 1.9 % and 4.1 %, respectively when dispersing 2 % of the Cu nanoparticles compared to the water-based cooling. The study further concluded that applying Cu-based nanofluid led to better enhancement in the system performance as compared to Al_2O_3-based nanofluid. Fudholi et al. [46] experimentally studied the use of TiO_2 nanofluid at 0.5 % and 1 % concentrations for a PVT system cooling under different solar radiation rates (specifically, 500, 700 and

900 W/m^2) and mass flow rate varying between 0.012 and 0.0255 kg/s. A theoretical model was created to compare the theoretical and experimental outcomes, showing an inverse proportion between high thermal and electrical efficiencies as the PV surface temperature increased at high solar radiation. Cooling by TiO_2 nanofluid at 0.1 % has enhanced the PVT system performance from 85 % to 89 % thanks to improved heat transfer coefficient. In contrast, cooling by water depicted enhancement from 60 % to 76 % at 0.0255 kg/s. Furthermore, the study indicated an exergy performance enhancement by 6.02 % at 1.0 % compared to cooling by water. Besides, the theoretical and experimental findings showed a high agreement, with an accuracy ranging from 97.6 % to 99.2 %. Another experimental and numerical investigation carried out by Sardarabadi and Passandideh-Fard [47] using deionized water, Al_2O_3, TiO_2, and ZnO nanofluids as a coolant to a PVT system at 0.2 % concentration. The system's electrical efficiency was assessed taking into account both the system's surface temperature and the fluid's output. Study outcomes revealed that employing TiO_2 and ZnO nanofluids has enhanced the PVT electrical performance more than Al_2O_3 and water. Besides, utilizing ZnO nanofluid showed superior thermal effectiveness compared to other fluids. Dashtbozorg et al. [48] investigated MXene/ethanol nanofluid included into heat pipe as a potential cooling fluid for a PVT system at 0.5 %, 1.0 % and 1.5 % concentrations. The study findings showed that employing MXene with 1 % concentration into ethanol has minimized the PV/T temperature by 19.21 °C, improving the electricity output by 1.62 W compared to water as a cooling fluid. Furthermore, the study indicated that the optimum PVT inclination angle was 30°, with 50 % filling ratio to obtain the highest performance.

Recent literature studies have reported that hybrid nanofluids are generally more effective than single-based cooling nanofluids in various solar systems [49]. In this regard, several research works were conducted on PVT systems, utilizing the remarkable thermal advancements of hybrid nanofluids. For instance, Sharaby et al. [50] experimentally employed multi-walled carbon nanotube/ zinc oxide (MWCNT-ZnO)-based hybrid nanofluid to cool three PVT modules, compared to an uncooled and water-cooled PV module. The study explored the module energy and exergy efficiency under 0.156 kg/min mass flow rate and a 0.1 % MWCNT-ZnO concentration. As a general outcome, the study displayed that employing MWCNT-ZnO hybrid nanofluid has notably augmented the PVT electrical efficiency by 16.8 % over the water-cooled module, while the thermal efficiency of the MWCNT-ZnO nanofluid and water-cooled modules were 51.3 % and 45.5 %, respectively compared to the uncooled PV module. Besides, the PVT exergy efficiency was advanced using MWCNT-ZnO hybrid nanofluid more than the water-cooled module by 7 %, and by 27 % more than the uncooled PV module along with 3.5 % entropy generation reduction and exergy destruction than the base (uncooled) PV module. Kazemian et al. [51] employed various hybrid nanofluids, namely MWCNT-Al_2O_3, MWCNT-SiC, G-Al_2O_3, and G-SiC-based water, into a connected PVT system and thermal collector in series. System evaluation was conducted concerning the fundamental principles of the 1st and 2nd thermodynamics laws. Through the analysis of entropy production, valuable insights were attained regarding the system's efficiency and performance. This assessment has comprehended the energy dissipation and possible enhancements inside the system utilizing thermodynamic rules that offer a thorough method for maximizing the system's performance. Inclusively, the MWCNT-SiC nanofluid reached the best performance, achieving thermal/electrical efficiency of about 56.55 %/13.8 %, and high entropy generation. Hooshmandzade et al. [52] installed an aluminium plate and copper tube heat exchanger on a PV module's rear side, and fibreglass was utilized to fill the pores in indoor and outdoor experiments. The electrical and thermal efficiencies of the proposed system were assessed considering the use of SiO_2-Al_2O_3 hybrid nanofluid at 0.5 %-0.5 % mixing ratio and their single nanofluids. The research findings disclosed superior performance for SiO_2-Al_2O_3 over single nanofluids, in which the PVT thermal and electrical efficiencies were enhanced by 65.05 % and 13.17 %, respectively under outdoor conditions, while the increase was about 65.08 % and 11.47 %, respectively for the indoor experiments. Comparatively, cooling by pure water has increased the overall PVT system performance by 48.54 % and 63.26 %, respectively while utilizing hybrid nanofluid has improved the overall efficiency by about 68.09 % and 75.26 % for indoor and outdoor experiments, respectively. A summary of literature studies and their key findings is reported in Table 1.

The existing studies have presented notable findings for PVT systems, employing various nanofluids all around the world. However, most investigations considered the thermal contribution of single nanofluids to improve the PVT performance. Besides, limited researchers have discussed energetic and exergetic analysis of PVT performance evaluation, giving an incomplete view of the technology. Consequently, this research aims to comparatively investigate the energetic and exergetic efficiencies of a PVT system employing single and hybrid nanofluids. Besides, the essential thermofluidic parameters, such as the heat transfer coefficient, Nusselt number, Reynolds number, and pressure drop were presented and discussed under various nanofluid concentrations. Therefore, a 3D model for a validated PVT module was numerically simulated using ANSYS Fluent software, in which Fe_2O_3/water (single nanofluid) and TiO_2-Fe_2O_3/water (hybrid nanofluid) fluids were investigated for various concentrations. The findings attained are believed to offer a good starting point for further future research to develop efficient and sustainable solar energy systems.

This work consists of four sections, as follows:

- Section 1 indicates the research actuality, scope, literature gaps, and work novelty,
- Section 2 presents the numerical model and evaluation approach, involving the model components, nanofluids employed, energy, exergy analysis, PVT geometry, assumptions, boundary conditions, and model validation,
- Section 3 highlights the results and their discussion, including a comparison with previous studies,
- Section 4 presents the conclusions derived from numerical results, limitations of current work and some notes for future studies.

2. Numerical model and evaluation approach

2.1. Model components

The numerical model adopted in this research is composed of a polycrystalline PV module (nominal output power of 50 W) integrated with a heat exchanger, and examined under the weather conditions in Miskolc City, Hungary. The system consists of a serpentine-shaped tube heat exchanger placed on a copper plate and positioned on the PV module's rear surface to cool the PV module by collecting surplus heat. Fig. 1 illustrates the PVT module and its components. The serpentine-shaped tube heat exchanger is characterized by a dense layout of tubes distributed on the absorber plate, increasing the heat exchange area and heat transfer efficiency. This arrangement could increase heat conduction between the contact regions (tubes and absorbing plate), and heat convection between (the tube's wall and circulating fluid), increasing the heat removal from PV cells. Table 3 shows more details about the properties of the PVT heat exchanger.

2.2. Nanofluids

Nanofluids-based Iron oxide (Fe_2O_3) nanoparticles and titanium oxide-iron oxide (TiO_2-Fe_2O_3) nanocomposite were presented in the current study as coolants. These metal oxides were adopted in this study due to their high thermal properties reported in the literature, availability with cost-effectiveness, and overlooked application in a hybrid form for PVT cooling. Besides, these metal oxides were stable during preparation and economically feasible, according to our earlier

Table 1
Summary of literature studies presented in the current research.

Researchers	Study type	Nanofluid type (concentration %)	PVT configuration	Main findings
Chen et al. [41]	Numerical	Al_2O_3/water (1 %, 3 % and 5 %)	The PVT module is provided with fluid flow pipes.	• The PVT average temperature was reduced by a maximum of 8.92 ℃ at 5 % concentration. • The PVT efficiency was increased by 12.36 % at a 5 % concentration of Al_2O_3/water, compared to a standard PV module.
Venkatesh et al. [42]	Experimental	Graphene nanoplatelets (GnP)/water (0.1 %, 0.2 % and 0.3 %)	The PVT module with a finned multi-block container of phase change material.	• The PV/T energy efficiency was improved by a maximum of 23 %.
Menon et al. [43]	Experimental	CuO/water (0.05 %)	An unglazed PVT combined a serpentine coil mounted on a sheet and thermal absorber.	• The PVT thermal efficiency cooled by the nanofluid reached 71.17 %, against 58.77 % when cooling by water.
Nasrin et al. [44]	Experimental and numerical	MWCNT/water (0 %, 0.3 %, 0.6 % and 1 %)	The PVT attached heat collection pipes from the rear side and combined them with a centrifugal pump and a radiator for heat dissipation.	• Total PVT performance was improved using MWCNT/water by 3.81 numerically and by 4.11 % experimentally compared to water-based fluid.
Hissouf et al. [45]	Numerical	Cu and Al_2O_3-based water (0 %, 0.01 %, 0.02 %, 0.03 % and 0.04 %)	The PVT supplied with a sheet and serpentine tube.	• Cu/water nanofluid showed a better performance enhancement than Al_2O_3/water. • Cu/water nanofluid improved the thermal and electrical efficiencies by 4.1 % and 1.9 % respectively, over water.
Fudholi et al. [46]	Theoretical and experimental	TiO_2/water (0.5 % and 1 %)	A PVT is provided with a unilateral channel for the fluid flow.	• The PVT energy efficiency attained at 1 % nanofluid and 0.0255 kg/s mass flow rate was 85 % − 89 %, compared to 60 %-76 % achieved by water cooling. • The PVT exergy efficiency was increased by 6.02 % over that cooled by water under the same concentration and mass flow rate.
Sardarabadi and Passandideh-Fard [47]	Experimental and numerical	Al_2O_3, TiO_2 and ZnO-based water (0.2 % in experimental work, and from 0.05 % to 10 % in the numerical work).	The PVT was provided with a sheet and tube collector.	• Increased metal oxide concentration from 0.05 % to 10 % has improved the PVT thermal performance by four times.
Dashtbozorg et al. [48]	Experimental	MXene/ethanol (0.5 %, 1.0 % and 1.5 %)	The PVT provides an array of two-phase closed heat pipes.	• The PV/T temperature was minimized by 19.21 °C using MXene/ethanol at 1 %, and the electricity output was augmented by 1.62 W compared to the water cooling fluid.
Sharaby et al. [50]	Experimental	MWCNT-ZnO/ water (0.1 %)	The PVT is provided with a serpentine absorbing sheet and tube.	• The PVT electrical efficiency was augmented by 16.8 % over the water-cooled module employing the nanofluid. • The PVT thermal efficiency using MWCNT/ZnO and water-cooled modules were 51.3 % and 45.5 %, respectively compared to the uncooled PV module. • The PVT exergy efficiency was advanced using MWCNT/ZnO hybrid nanofluid by 7 %, and 27 % more than the water-cooled and uncooled PV modules.
Kazemian et al. [51]	Numerical	MWCNT-Al_2O_3, MWCNT-SiC, G-Al_2O_3, and G-SiC-based water (1 %: 1 %)	The PVT was connected in series with a thermal collector.	• MWCNT-SiC hybrid nanofluid achieved the highest electrical energy efficiency of 13.85 %, and thermal energy efficiency of 56.55 %.
Hooshmandzade et al. [52]	Experimental	Single nanofluid: SiO_2 and Al_2O_3 (0.1 %, 0.3 %, and 0.5 %), Hybrid nanofluids: SiO_2-Al_2O_3 (0.1 %-0.1 %, 0.3 %- 0.3 % and 0.5 % − 0.5 %).	The PVT is provided with an aluminium plate and copper tube heat exchanger.	• Under outdoor conditions, the PVT thermal and electrical efficiencies were enhanced by 65.05 % and 13.17 %, respectively, while increased by 65.08 % and 11.47 %, respectively for the indoor experiments. • The PVT overall efficiency using SiO_2-Al_2O_3 has improved by 68.09 % and 75.26 % for indoor and outdoor experiments, respectively.

experimental research [53]. Hybrid nanofluids are characterized by high thermophysical properties (increased thermal conductivity, specific heat and low density) which positively improve the PVT energy and exergy efficiencies more than single nanofluids [54]. Economically, it was reported that employing hybrid nanofluids achieved better economic feasibility with a shorter payback period [53,55], making them an effective option for cooling applications. Besides, the low density of hybrid nanomaterials helps increase the stability of hybrid nanofluids more than single nanomaterials, giving another desired property [56]. The real thermal and physical characteristics of TiO_2-Fe_2O_3 nanocomposites were examined at the University of Miskolc, while those of the Fe_2O_3 nanomaterials were considered from previous studies. Nanofluids' thermophysical properties are determined using equations (1–5) [57–60]. Table 2 lists the thermophysical characteristics of nanomaterials delivered during modelling.

The density of of nanoparticle (ρ_{np}), nanofluid (ρ_{nf}), and the base

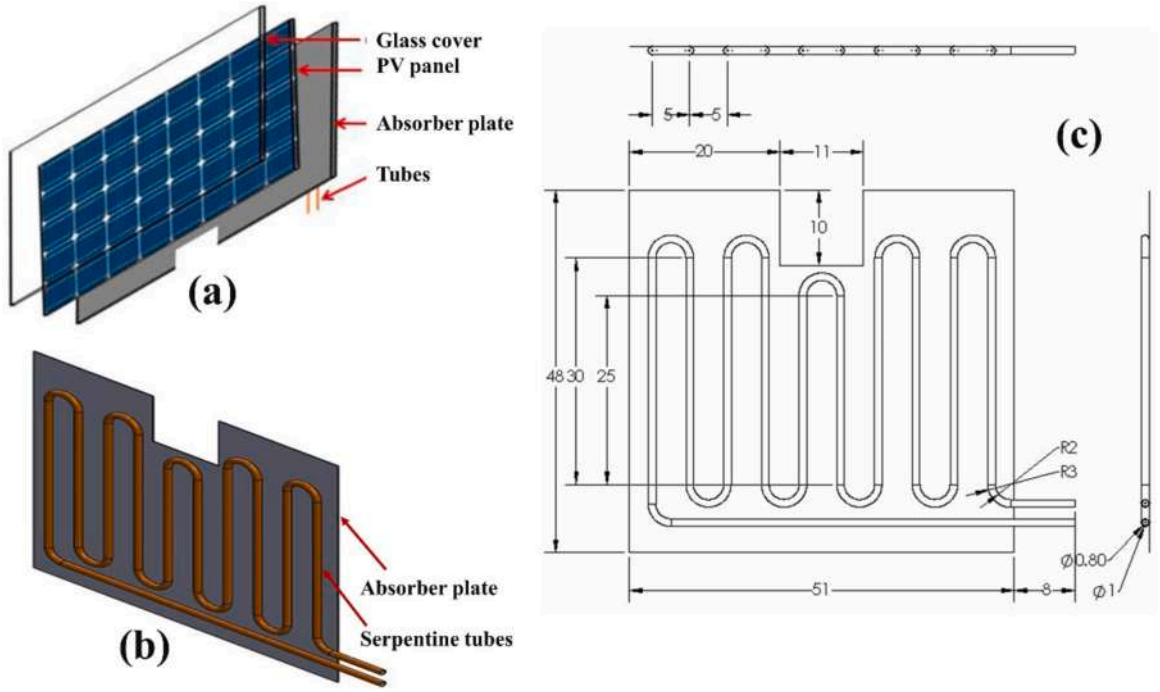

Fig. 1. (a) PVT layers, (b) absorbing plate and serpentine tubes, (c) schematic view of PVT serpentine tubes with dimensions.

Table 2
Thermophysical properties of nanomaterials.

Property	Unit	TiO_2-Fe_2O_3	Fe_2O_3 [61]
Density	kg/m^3	3473	5240
Thermal conductivity	W/m·K	75.32	20
Heat capacity	J/kg·K	1321	650

fluid (ρ_{bf}) was calculated by Eq. (1), as follows:

$$\rho_{nf} = \phi \cdot \rho_{np} + (1-\phi)\cdot \rho_{bf} \tag{1}$$

where ϕ is the nanoparticles concentration, which can be computed from Eq. (2). Moreover, m_{bf} and m_{np} signifies the mass of base fluid and nanoparticles. Besides, the thermal conductivity of nanoparticles (k_{np}), nanofluid (k_{nf}), and the base fluid (k_{bf}) was calculated by Eq. (3).

$$\phi = \left[\frac{\frac{m_{ap}}{\rho_{np}}}{\frac{m_{np}}{\rho_{np}} + \frac{m_{bf}}{\rho_{bf}}} \right] \times 100 \tag{2}$$

$$\frac{k_{nf}}{k_{bf}} = \frac{k_{np} + 2k_{bf} + 2\varnothing\left(k_{np} - k_{bf}\right)}{k_{np} + 2k_{bf} - \varnothing\left(k_{np} - k_{bf}\right)} \tag{3}$$

The specific heat of the nanofluid ($C_{p,nf}$), nanomaterial ($C_{p,np}$), and the base fluid ($C_{p,bf}$) was calculated by Eq. (4), while the nanofluid viscosity was calculated by Eq. (5), as follows:

$$C_{p,nf} = \frac{\phi\cdot\left(\rho_{np}\cdot C_{p,n}\right) + (1-\phi)\cdot\left(\rho_{bf} C_{p,bf}\right)}{\rho_{nf}} \tag{4}$$

$$\mu_{nf} = \frac{\mu_{bf}}{(1-\phi)^{2.5}} \tag{5}$$

2.3. Energy analysis

The electrical performance of PVT could be quantified as the input energy ($E_{in} = P_{pv}\cdot FF$) divided by the output energy ($E_{out} = S\cdot A_c$). The electrical efficiency is a crucial indicator to assess the system performance, which could be calculated from Eq. (6) [62].

$$\eta_{ele} = \frac{E_{out}}{E_{in}} \tag{6}$$

where P_{pv}=$I_{pv}\cdot V_{pv}$ is the electrical power W, I_{pv} is the current A, V_{pv} is the voltage V, and FF is the fill factor which could be determined from Eq. (7) [62]. S is the incident solar emissions W/m^2, while A_c is the PVT system's area in m^2.

$$\mathrm{FF} = \frac{V_{PV} \times I_{PV}}{V_{Oc} \times I_{Sc}} \tag{7}$$

The enhancement in the PVT thermal efficiency depends on the heat transfer from the PV rear surface to the cooling fluid inside tubes over the absorbing plate. This transfer can be quantified by Eq. (8) [63].

$$\eta_{th} = \frac{\dot{m} C_p (T_{\mathrm{out}} - T_{\mathrm{in}})}{\mathrm{AS}} \tag{8}$$

where $\dot{m}$ is the mass flow rate (L/min), C_p is the fluid's heat capacity (J/kg·K), T_{in} and T_{out} are the inlet, and outlet cooling fluid temperatures (°C). The entire performance of the PVT system is determined by the combined thermal and electrical efficiencies, using Eq. (9) [64].

$$\eta_{ov} = \eta_{el} + \eta_{th} \tag{9}$$

Nanofluid thermophysical characteristics influence the heat transfer rate, affecting the PVT thermal and electrical efficiencies. Besides, nanofluids' flow pattern in tubes affects the heat transfer rate from the PV module. These flow patterns are predicted by quantifying the Reynolds number, which can be determined by Eq. (10) [65].

$$\mathrm{Re}_{nf} = \frac{4\dot{m}}{\pi \mu_f D_h} \tag{10}$$

where μ_f is the fluid viscosity and D_h is the hydraulic diameter. Eq. (11) determines the Nusselt number, the ratio of the convective and conductive heat transfer [66].

$$Nu_{nf} = \left(\frac{hD_h}{K_{nf}}\right) = \frac{\dot{m}C_p\left(T_{h,i} - T_{h,\rho}\right)}{A\left(T_{avg} - T_w\right)} \times \frac{D_h}{K_{nf}} \quad (11)$$

h is the heat transfer coefficient, and T_w is the wall tube mean temperature. The friction factor is an intrinsic parameter that influences the fluid pressure drop with a Reynolds number change, which occurs due to a viscosity growth resulting from the rise in Nanomaterials' volume concentration in the base fluid. Both fraction factor and pressure drop are determined by Eq. (12) and (13). [67,68]

$$f = [1.58\ln Re - 3.82]^{-2} \quad (12)$$

$$\Delta P = \frac{f\rho_f L}{2D_{tubes}}\left(\frac{4\frac{m_f}{n}}{\rho_f \pi D^2}\right)^2 \quad (13)$$

where n is the number of heat exchanger tubes and L is their length.

2.4. Exergy analysis

Exergy analysis is a crucial concept for evaluating the energy efficiency generated by the system when it is in thermodynamic equilibrium with its surroundings [69]. The efficiency of electrical and thermal exergy is affected by the system's amount of exergy inputs (solar exergy and exergy of mass flow) and exergy outputs (electrical exergy, thermal exergy, and exergy destruction). The solar exergy ($\dot{E}x_{solar}$) computed using Eq. (14) [70] considering the amount of solar radiation absorbed by the PVT, and the exergy of mass flow is the inlet cooling fluid to the system.

$$\dot{E}x_{solar} = S\left(1 - \frac{T_{amb}}{T_{sun}}\right) \quad (14)$$

where T_{amb} and T_{sun} are the ambient and sun temperatures (5800 K) [71]. Consequently, the PVT energy efficiency in terms of both thermal and electrical performance was calculated by Eq. (15) and (16) [72].

$$\eta_{\dot{E}x_{ther}} = \frac{\dot{m}C_{p,nf}\left[\left(T_{f,out} - T_{f,in}\right) - T_{amb}\ln\left(\frac{T_{f,out}}{T_{f,in}}\right)\right]}{S\left(1 - \frac{T_{amb}}{T_{sun}}\right)} \times 100 \quad (15)$$

$$\eta_{\dot{E}x_{ele}} = \frac{P_{pv}FF}{S\left(1 - \frac{T_{amb}}{T_{sun}}\right)} \times 100 \quad (16)$$

$T_{f,in}$ and $T_{f,out}$ are the input and output fluid temperatures, respectively.

2.5. PVT geometry, assumptions, and boundary conditions

The suggested PVT model comprises a glass protector, PV modules, and an absorbing plate, which is in direct contact with a serpentine tube heat exchanger. The geometry was generated using SolidWorks which is introduced to the ANSYS 19.2 software. The numerical model characteristics are presented in Table 3. The solar emission collected by the absorbing plate was made of copper and relies on the transmittance of the section of cover glass and the PV module's absorptivity, which can be understood as a constant heat flux [73].

Table 3
Characteristics of model components.

Cover glass	PV module	Absorber	Tubes
Emissivity: 0.88	*Riser's number modules*: 60 *Area*: 0.355 m^2 *Absorptance*: 0.9 *Emissivity*: 0.88 η_r = 15 %, β_r= 0.0045 °C^{-1}	*Area*: 0.2928 m^2 *Thickness*: 0.002 *m* *Material*: Copper C_p = 381 J/kg K, k = 387.6 W/m K, ρ = 8978 kg/m^3	*Tube length*: 5 *m* *Tube thickness*: 0.001 *m* *Outer diameter*: 0.01 *m* *Material*: Copper

The following assumptions have been applied during the simulation:

i. Fluid flow is steady-state, uniform and incompressible,

ii. A rate of the solar radiation falling on the PV module is converted into electrical energy, while the other rate warms up the PV module.

iii. Nanoparticles and base fluid are assumed as a single fluid in computations (a common concept in the literature [74–76]).

iv. The heat loss by radiation is disregarded as a result of the PVT system temperature reduction.

v. The absorbing plate's bottom surface is thermally insulated from the surface tubes.

vi. The PVT system components are in ideal contact. Therefore, the temperature is consistent across all layers.

Concerning the assumptions presented above, the governing equations of energy, continuity, and momentum (Eqs. 18–20) are utilized in the simulation [77]. These equations succinctly represent the boundary conditions for the current scenarios.

Energy equation

$$\nabla\cdot\left(\rho_{nf}U_{nf}C_{p_{nf}}T\right) = \nabla\cdot\left(k_{nf}\nabla T\right) \quad (18)$$

Continuity equation

$$\nabla\left(\rho_{nf}U_{nf}\right) = 0 \quad (19)$$

Momentum equation

$$\nabla\cdot\left(\rho_{nf}U_{nf}U_{nf}\right) = -\nabla P + \nabla\tau + \rho_{nf}g \quad (20)$$

The finite volume approach is employed to solve these equations. The heat flux was specified based on the boundary conditions, while the fluid temperature and its velocity at the inlet were specified. Then, the turbulent intensity specification method was adopted considering Eq. (20) and the hydraulic diameter. The fluid flow at the tube output is considered to be fully developed. The flow regime was analyzed using the k-epsilon model. PVT systems typically involve forced convection to flow the fluid within channels or ducts, exhibiting turbulence, in most cases, due to high Reynolds numbers. The fluid flow is often characterized by boundary layer separation, heat transfer across surfaces, and varying temperature gradients. Thereby, the k-epsilon turbulence model is appropriate for high Reynolds numbers and efficient simulation time as it offers an efficient balance between computational cost and accuracy. The second-order upwind is employed by available spatial discretization schemes from the CFD environment for the diffusion, convection and radiation terms. The PVT system component properties and thermophysical parameters of nanofluids were adopted from the software database. The rear side of the absorbing plate has adiabatic boundary conditions, as does the external tube surface, with zero heat flux. The heat rate generated on the PVT surface equals the solar radiation absorbed by the system, assuming that this heat is transferred to the surroundings in a convective-radiative form.

Meshing is an essential metric to obtain accurate results from CFD simulations, notwithstanding solving times becoming longer when the mesh is small [78]. However, the three-dimensional mesh generation is significant to the CFD simulation of the absorbing plate and attached tubes model. Fig. 2 shows the mesh shape with suitable aspect ratios, which improved the quality of model meshing with 0.1 mm element size and a total of 779,755 elements, which helped reduce the errors. Meshing the PVT model helps optimize the simulation results and its accuracy. The meshing process was performed with high smoothness, one of the parameters required to assess the quality meshing of the PVT model. The temperature gradient (in Fig. 4) displays no substantial difference, confirming the optimal number of model meshing. It was observed that no more improvement was attained after 779,775

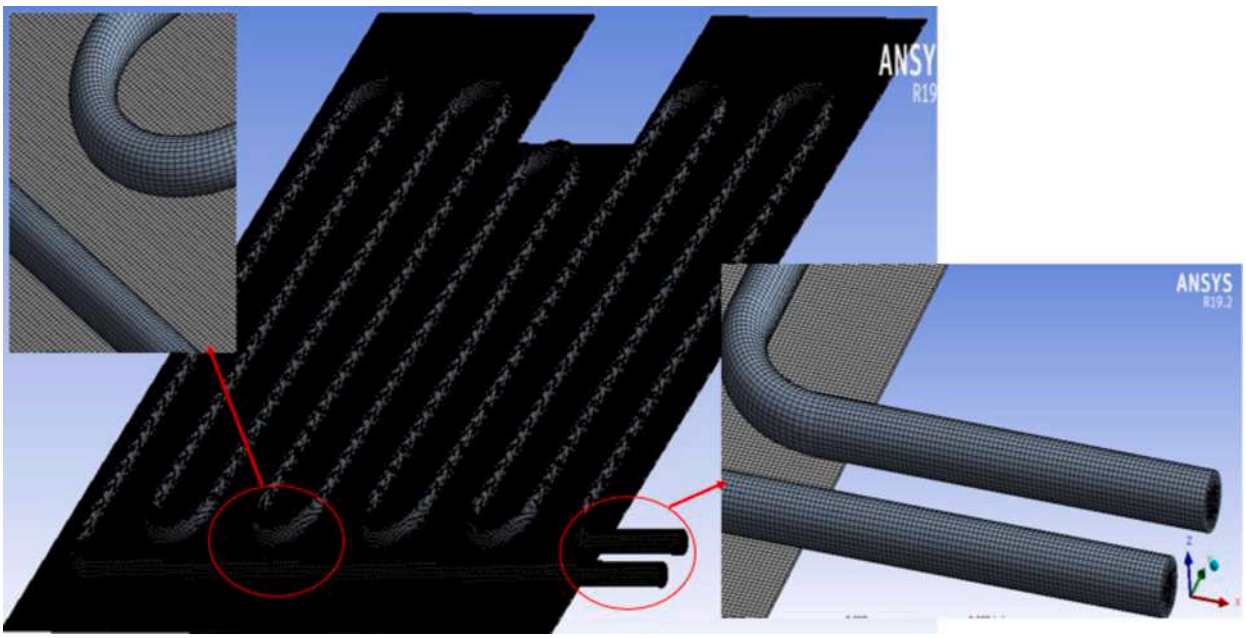

Fig. 2. Model mesh as presented in the ANSYS software.

elements, while the meshing process was performed with high smoothness.

A convergence criterion indicates subsets that specify the convergence of functions based on particular conditions, which continue until the convergence is fulfilled. In the current study, the solution convergence criterion was 10^{-8}, 10^{-7}, and 10^{-6} for energy, continuity and momentum equations. The convergence criteria obtained from the simulation determined the numerical stability of the results obtained.

The gravitational acceleration is a crucial factor that influences the convection in terms of buoyancy force (depending on the tilt angle of the system setup). This feature has been enabled in the simulation and is specified in the equations (24–26) [77]. The Dittus-Boelter equation was employed to calculate the turbulent flow characteristics with a smooth surface and fully turbulent conditions, as per Eq. (22).

$$I = 0.16\,Re^{\frac{1}{8}} \tag{21}$$

$$Nu = 0.023\,Re^{\frac{4}{5}}Pr^{n} \tag{22}$$

$$Pr = \frac{C_{p\mu}}{k} \tag{23}$$

$$g_x = -gSin\theta \tag{24}$$

$$g_y = 0 \tag{25}$$

$$g_z = +g\cos\theta \tag{26}$$

2.6. PVT model validation

The numerical PVT model has been validated for more reliability considering the outcome of our earlier experimental studies that were performed for the same PVT system using CuO and Fe_2O_3 nanofluids with 0.3 % volume concentration [55,79]. Consequently, similar environmental operation conditions and PVT model geometry were approved to determine the temperature drop, energy, and exergy efficiencies as a reference for validating numerical results. The experimental results when the CuO-based nanofluid was employed as a working fluid showed a 10.06 °C in the PVT temperature declination, while numerical results achieved a 10.34 °C (about 0.28 °C difference). Moreover, numerical simulations displayed a PV module temperature reduction of 15.33 °C when cooling by TiO_2-CuO nanofluid, while experimental results indicated a 14.5 °C temperature decrement (0.83 °C temperature difference). Fig. 3 reveals the experimental and numerical results performed in the current numerical model considering the thermal/electrical efficiencies and thermal/electrical exergy efficiencies at the same volume concentration. The figure discloses an acceptable agreement between numerical and experimental outcomes, in which the maximum thermal efficiency deviation was 3.59 % employing CuO nanofluid, while employing TiO_2-CuO nanofluid verified 2 %, only. Moreover, the maximum deviation of electric efficiency was 3.1 % when CuO nanofluid was employed against 3.14 % attained for TiO_2-CuO hybrid nanofluid. Fig. 3 (b) displays that the variation in the thermal and electrical exergy efficiencies for numerical and experimental results using CuO and TiO_2-CuO nanofluid also showed good agreement with no more deviation than 4 %. Regarding thermal exergy, it could be observed that the deviation was about 4 % and 3.98 % when CuO and TiO_2-CuO nanofluids were employed. Besides, the deviation between numerical and experimental electrical exergy efficiencies was 4.13 % and 4.38 % employing CuO and TiO_2-CuO nanofluids, respectively.

3. Results and discussions

3.1. Temperature variation of numerical model

Fig. 4 (a) demonstrates the gradual heat transfer in tubes contacting the absorbing plate under the nanofluid usage, in which a similar trend was observed when cooling the PVT by Fe_2O_3 and TiO_2- Fe_2O_3 nanofluids. The fluid temperature increment at the tube end is caused by the buildup of heat as the nanofluid flows through the serpentine tubes. The heat accumulation arises from the ongoing absorption of thermal energy by nanoparticles. As a result, the fluid leaves the tube at a higher temperature, indicating the effective transmission of heat inside the heat exchanger system. The temperature variation on the absorbing plate was quantified at a 14.8° tilt angle for a nanofluid concentration of 0.2 % entering the input tube at 0.323 m/s velocity, 295 K initial temperature, and 912 W/m^2 solar radiation intensity. The nanofluid cooling improves the PVT's overall efficiency and durability by helping to prevent overheating. Cooling nanofluid lowers the PV modules' temperature as a

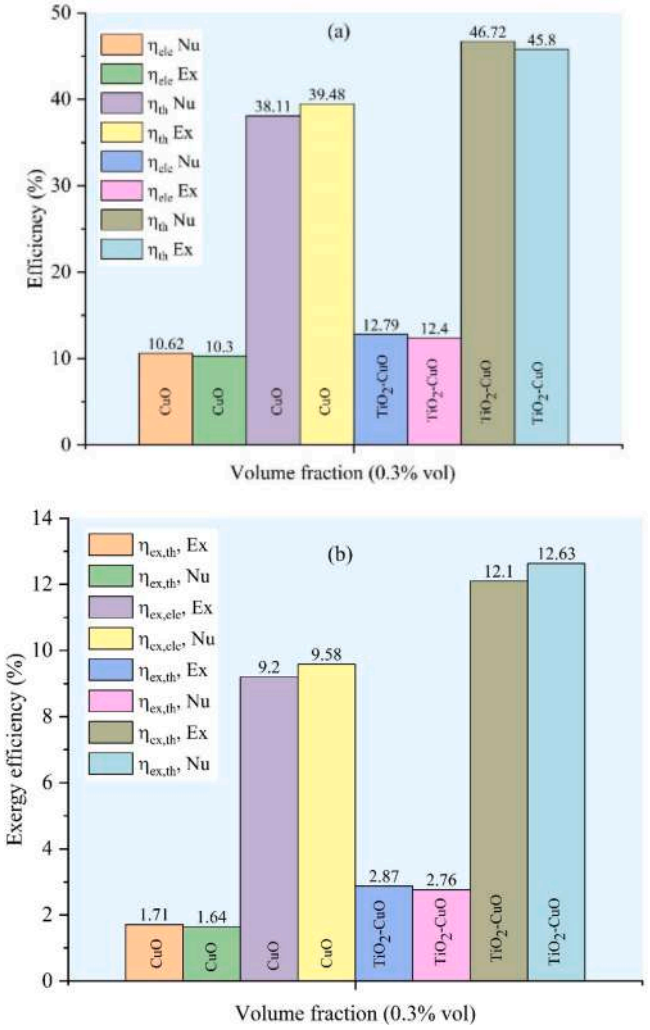

Fig. 3. Validation of PVT system with experimental results (a) energy efficiency, (b) exergy efficiency.

result of the absorbing plate temperature reduction, and then, its temperature increases continuously as passing within the serpentine tube, extracting thermal energy from the PV modules via the absorbing plate. Fig. 4 (b) depicts the thermal characteristics of the cooling fluid as it enters the input tube under low-temperature conditions. As could be observed, the cooling fluid temperature was increased gradually, reaching its maximum at the outlet tube end since the heat transmission occurs in a conductive way between the absorbing plate and tubes and, in a convective way to the nanofluid. This gradual increase in temperature indicates the presence of effective heat transmission mechanisms inside the system. The temperature contour designated a gradual rise in temperature from the tube wall towards the fluid stream and the highest temperature value was observed at the connection part between the heat exchanger and the absorbing plate.

3.2. Energy analysis results

The impact of nanoparticle concentration on the PVT system's maximum, average, and minimum temperatures is indicated in Fig. 5. In general, the gradual increase in nanoparticle concentration in water has improved the nanofluid thermal conductivity, enhancing the absorbing heat from the PVT system. Employing TiO_2-Fe_2O_3 hybrid nanofluid to cool the PV module has decreased the temperature more than using Fe_2O_3 nanofluid. The nanocomposite's thermal properties and surface area have been enhanced by loading TiO_2 NWs over Fe_2O_3 NPs. This has led to a progressive enhancement in the nanofluid's performance by improving heat transfer between the absorbent plate and the rear surface of the PV module. A maximum temperature of 53.8 °C was attained for the uncooled PV module. Cooling the PVT system with Fe_2O_3-based nanofluids at 0.2 % and 0.3 % has lowered the maximum temperature by 11.68 % and 13.26 % over the uncooled PV module. Cooling with DI water has minimized the PVT temperature by 4.06 % compared with the reference PV module without cooling. Fig. 5 displays the PVT temperature verified at 0.2 % and 0.3 % concentrations. In comparison to the PVT cooling by DI water, the PVT temperature decreased gradually as the nanoparticle concentration increased in the base fluid. Conversely, the PVT temperature was significantly reduced by employing the hybrid TiO_2- Fe_2O_3 nanofluid as a result of its improved thermophysical characteristics. Employing TiO_2-Fe_2O_3-based nanofluid with 0.2 % and 0.3 % concentrations has decreased the PVT temperature more than using Fe_2O_3 nanofluid and DI water. Consequently, employing TiO_2-Fe_2O_3-based hybrid nanofluid has significantly decreased the PV temperature by 18.77 % and 21.12 % in comparison with the uncooled case.

The quantitative PVT performance is demonstrated by the system efficiency, which incorporates both electrical and thermal efficiencies. Fig. 6 shows the PVT efficiencies at various cooling fluids and concentrations. As can be observed in the figure, employing Fe_2O_3-based nanofluid has declined the PVT temperature at various concentrations as compared to the cooling by DI water. Besides, the excess heat absorbed from the PVT rear surface was maximized due to enhanced fluid characteristics, improving the PVT electrical efficiency gradually. Quantitatively, the PVT electrical efficiency was improved by about 66.19 % when using Fe_2O_3 nanofluid in comparison with DI water. Employing Fe_2O_3-based nanofluid has improved the absorptance of surplus heat from the PVT and enhanced its thermal efficiency, reaching a peak value of 34.5 % at a 0.3 % concentration. In contrast, DI water showed a thermal efficiency of about 24.38 % only.

The electrical and thermal efficiencies were significantly enhanced by employing the hybrid nanofluid at various volume concentrations. In this regard, incorporating TiO_2-Fe_2O_3 nanocomposite into DI water has substantially reduced the PVT temperature, superior to the effect of using Fe_2O_3 nanofluid. Furthermore, TiO_2-Fe_2O_3-based nanofluid has improved the PVT electrical efficiency by 82.11 % at 0.3 % concentration, while the water usage yielded 7.1 %. Conclusively, enhanced thermophysical characteristics of TiO_2-Fe_2O_3 nanofluid have augmented heat transfer from PVT and increased the thermal efficiency by up to 78.42 % at 0.3 %.

Fig. 7 illustrates the impact of Fe_2O_3 and TiO_2-Fe_2O_3 nanofluids at various concentrations on the Nusselt number, considering the Reynolds number as an independent variable. In general, the Nusselt number exhibited a gradual increase at increased Reynolds number due to nanoparticle presence. Dispersing Fe_2O_3 nanoparticles with 0.2 % and 0.3 % concentrations has amended the Nusselt number by 25.84 % and 31.75 %, respectively over the DI water usage. When the TiO_2- Fe_2O_3 nanocomposites are dispersed in the base fluid, the Nusselt number was augmented to 81.23 % at 90.64 % at 0.2 % and 0.3 % concentrations over the DI water. In this regard, it could be stated that higher Reynolds numbers have augmented Nusselt numbers which positively improved the heat transfer coefficient of TiO_2-Fe_2O_3 nanofluid.

Fig. 8 displays the effect of increased Reynolds number and nanofluid concentration on its heat transfer coefficient. The figure demonstrates that the heat transfer coefficient was improved as the Reynolds number augmented at various concentrations. Dispersing Fe_2O_3 to the host fluid at 0.2 % and 0.3 % has augmented the heat transfer coefficient by 15.06 % and 19.45 %, respectively over the DI water. Besides, the addition of TiO_2-Fe_2O_3 nanocomposite with these concentrations has enhanced the hybrid nanofluid heat transfer coefficient by 41.35 % and 47.53 %, respectively. Accordingly, the PVT surface temperature was decreased using nanofluids more than the water.

The TiO_2-Fe_2O_3-based hybrid nanofluid experienced an augmentation in the heat transfer coefficient resulting from superior thermal

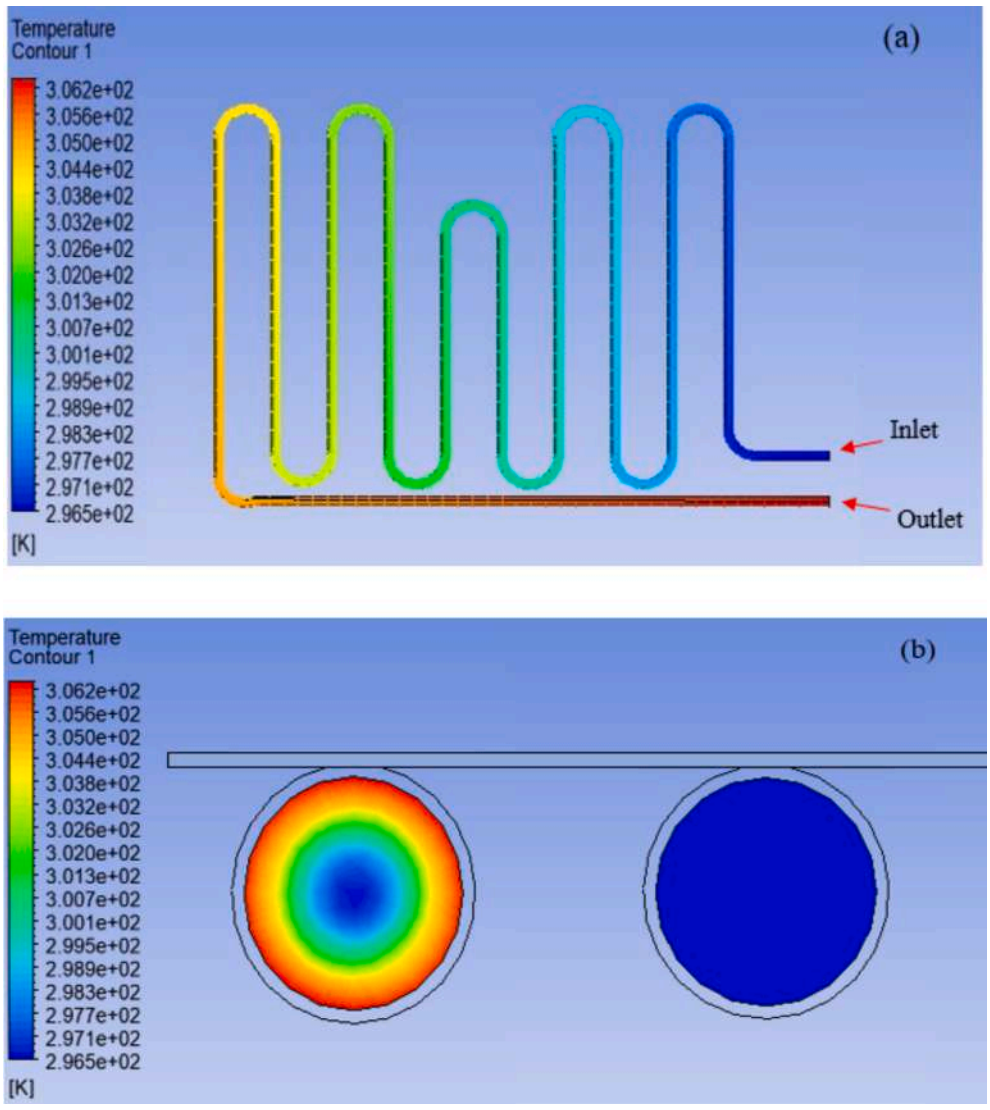

Fig. 4. Temperature distribution contour: (a) serpentine tube, (b) inlet and outlet tubes.

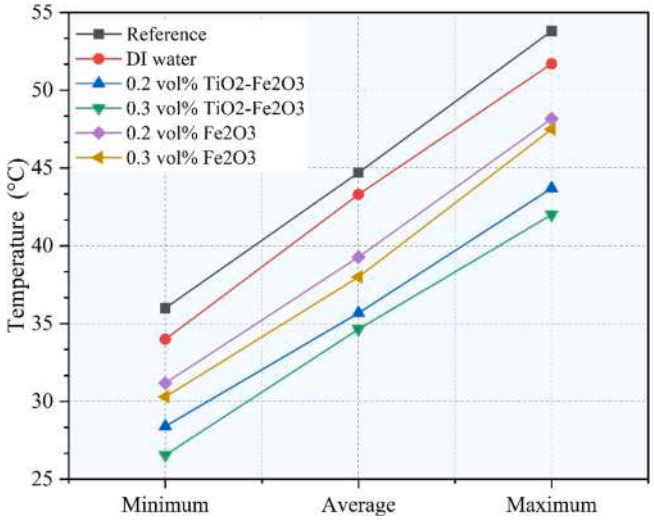

Fig. 5. Minimum, average and maximum temperatures of reference PV, DI water-cooled PVT and PVT system cooled by Fe_2O_3 and TiO_2-Fe_2O_3 nanofluids.

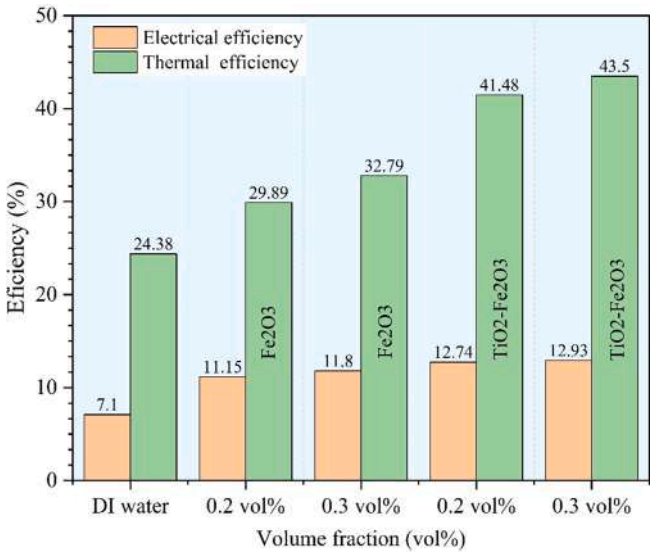

Fig. 6. Electrical and thermal efficiencies of the PVT system cooled by DI water, Fe_2O_3, and Fe_2O_3-TiO_2 nanofluids at different concentrations.

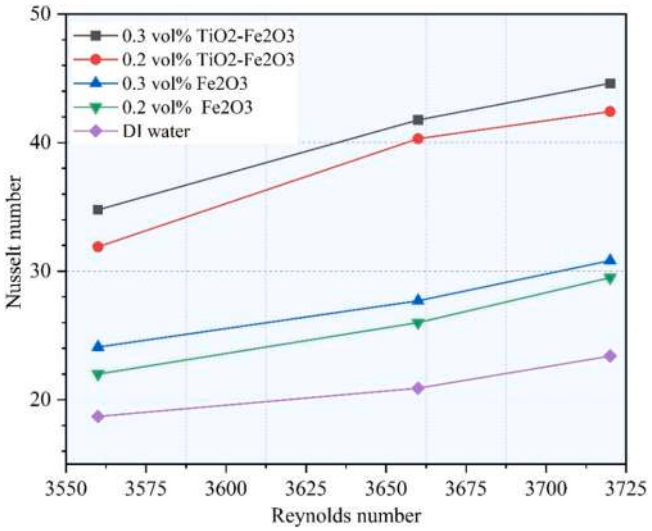

Fig. 7. Relationship of Reynolds number and Nusselt number for the PVT cooled by DI water and nanofluids at various concentrations.

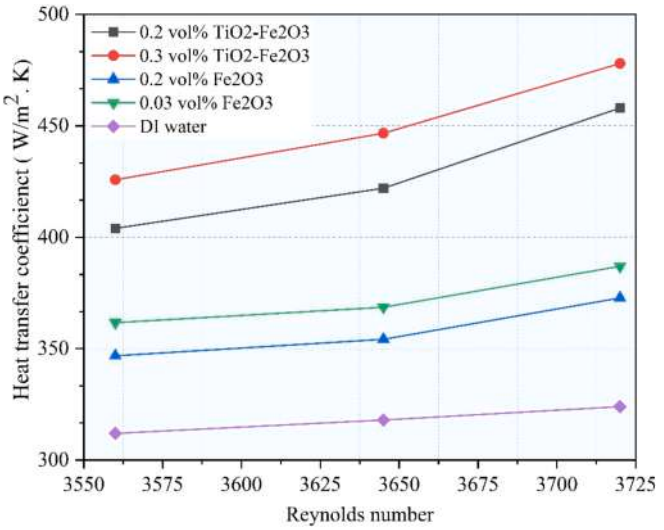

Fig. 8. Relationship of Reynolds number and heat transfer coefficient for the PVT cooled by DI water and nanofluids at various concentrations.

conductivity. However, the nanofluid density was augmented due to the higher volume concentration, which negatively influenced the pressure drop. Although the nanofluid's thermal conductivity has greatly improved the Nusselt number and heat transfer coefficient with increasing nanofluid concentration, the nanofluid density has slightly increased, affecting the pressure drop negatively. The nanofluid concentration significantly influences the heat conduction between the PV module rear side and the absorbing plate attached to tubes, and heat convection between tube walls attached to the absorbing plate and circulating nanofluids inside tubes. Consequently, increasing the nanoparticles concentration has increased the Nusselt number and improved the heat transfer coefficient of circulating nanofluids which increased the heat exchange.

The fluid pressure drop is affected by the fraction factor and Reynolds number. The fluid friction factor is influenced by the volume concentration of dispersed nanomaterials into host fluids, while the Reynolds number is affected by the circulated fluid viscosity. Accordingly, increasing the nanomaterials concentrations could achieve a high heat transfer coefficient, while raising friction factor and pressure drop. The effect of increased Reynolds number and nanofluid concentration on pressure drop is illustrated in Fig. 9. The figure findings indicate an augmentation in pressure drop with Reynolds number increment, affected by the higher density of the nanofluid compared with water. This behaviour is predictable due to the dispersing of Fe_2O_3 nanoparticles in the base fluid at various concentrations. As a result, the higher nanofluid concentration has incremented the pressure drop by 35.55 % when employing Fe_2O_3-based nanofluid at 0.3 % concentration. Correspondingly, immersing TiO_2- Fe_2O_3 nanocomposite in the water has resisted fluid movement, which increased pressure drop. The pressure drop in this case has increased by 62.9 % and 69.41 % respectively at 0.2 % and 0.3 % nanocomposite concentrations, over the water base fluid. Increasing dispersed nanomaterial concentration in the base fluid augments the fluid pressure drop due to increased nanofluids' density, even with an increased Reynolds number, requiring more power for pumping nanofluids. Moreover, when the nanomaterial size exceeds the optimal values leading to increased heat transfer augmentation with a penalty of rising pressure drop. Agglomeration and sedimentation of nanomaterials in the nanofluid due to gravity affect the heat transfer surface, increasing the pressure drop with rising power pumping [80].

3.3. Exergy analysis results

The system's thermal exergy performance is affected by several factors, including fluid output temperature, nanomaterials concentration, and fluid mass flow rate. The PVT exergy efficiency at Fe_2O_3 and TiO_2-Fe_2O_3 nanofluids cooling is presented in Fig. 10. As could be demonstrated, the presence of Fe_2O_3 nanoparticles and TiO_2-Fe_2O_3 nanocomposites in the water has gradually increased its thermal exergy compared to water. However, the thermal exergy performance was much inferior to the electrical exergy performance. This might be attributable to the slight discrepancy between the fluid temperature leaving the outlet and the surrounding ambient temperature, which was previously described in the literature [37]. Moreover, the PVT electrical exergy efficiency was augmented as nanofluid concentration increased and the heat transfer coefficient improved. Fig. 10 also shows a progressive increase in electrical exergy efficiency as the volume concentration increases, reaching the highest value of 10.24 % when employing Fe_2O_3 nanofluid at a volume concentration of 0.3 %, against 6.97 % when DI water is employed.

The figure also exhibits that employing TiO_2-Fe_2O_3 hybrid nanofluid with 0.2 % and 0.3 % has augmented the PVT electrical exergy by about 11.79 % and 12.62 %, respectively. However, employing TiO_2-Fe_2O_3 nanofluid has incremented the PVT electrical exergy efficiency by 69.26

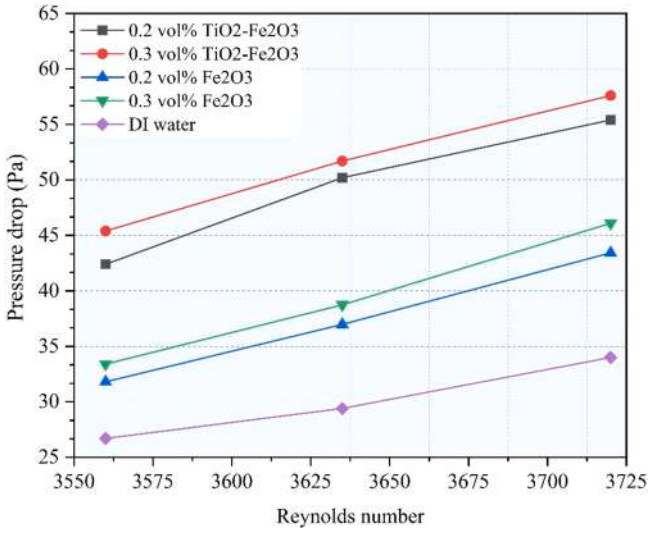

Fig. 9. Relationship of Reynolds number and pressure drop for the PVT cooled by DI water and nanofluids at various concentrations.

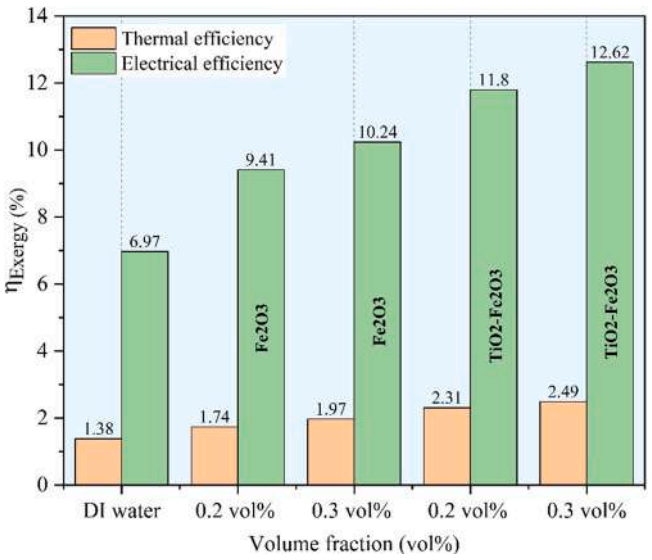

Fig. 10. Exergy efficiency of the PVT system cooled by DI water, Fe_2O_3, and Fe_2O_3-TiO_2 nanofluids at different concentrations.

% and 81.06 % at 0.2 % and 0.3 % nanocomposite concentration, respectively. The improvement in electrical energy efficiency has resulted in a significant increase in PVT total exergy over thermal energy efficiency. This might be attributed to the cooling fluid's high thermal conductivity, which enhanced heat transfer between the fluid and the tubes installed on the absorbent plate.

Table 4 compares the results obtained from the current study with the outcomes achieved in previous studies. Some factors were considered in the comparison, such as the nanofluid type, volume fractions, and the advancements in PVT efficiencies.

The comparison indicates the potential of TiO_2-Fe_2O_3/water hybrid nanofluids to improve the PVT system efficiencies compared to literature studies at different conditions. These findings may contribute to developing more efficient and sustainable solar energy systems. Besides, the significant outcomes of the proposed hybrid nanofluid may encourage the investigation of traditional metal oxides to produce thermally effective and cost-effective nanofluids.

4. Conclusions

Employed hybrid nanofluid for cooling PV cells is a novel methodology for improving the PVT system performance and highlights the potential of nanofluid as a cooling fluid. This work numerically investigates the influence of employing Fe_2O_3 and TiO_2-Fe_2O_3 nanofluids on the PVT energy and exergy efficiencies at 0.2 % and 0.3 % concentrations. The numerical outcomes demonstrated remarkable findings, which could be summarized as follows:

- Thermal properties of nanofluids improved when dispersing nanomaterials with 0.2 % and 0.3 % concentrations. However, high nanoparticle concentration (i.e., 0.3 %) helped reduce the PVT temperature by 13.26 %, and 21.12 %, employing Fe_2O_3 and TiO_2-Fe_2O_3 nanofluids.
- Improving the heat transfer coefficient by 19.45 %, and 47.53 % contributes to lowering the temperature between the absorptive plate and the PVT rear surface, increasing the electrical efficiency by up to 66.19 %, and 82.11 % using Fe_2O_3 and TiO_2-Fe_2O_3 nanofluid, respectively.
- Improved nanofluid thermal characteristics have increased heat absorption of the PVT, maximizing the thermal efficiency by 32.79 % and 78.42 % for the Fe_2O_3 and TiO_2-Fe_2O_3-based nanofluids, respectively.
- Regardless of enhanced fluid heat transfer and the Nusselt number by up to 31.75 % and 90.64 %, increasing nanoparticle concentration has augmented pressure drop by 35.55 %, and 69.41 %, respectively using Fe_2O_3 and TiO_2-Fe_2O_3-based nanofluids.
- Employing Fe_2O_3 and TiO_2-Fe_2O_3-based nanofluids has augmented the PVT thermal efficiency by up to 32.79 %, and 78.42 %, respectively, corresponding to 166.5 % efficiency improvement.
- Enhanced nanofluid thermophysical properties have promoted the PVT electrical exergy by up to 12.62 % for the hybrid nanofluid, while single nanofluid attained 10.24 %.

The results achieved in the current work are limited to the proposed PVT system and nanofluid types, which may be feasible for small installations for domestic applications in specific locations. Therefore, more investigations of mega PVT systems are still needed since they require more nanofluids quantities and cost-effective heat exchanger design. Future studies could consider the heat exchanger design and synthesis of low-cost hybrid nanomaterials with low density. Besides, integrating thermal energy storage materials, such as phase change materials, has a promising future in regulating the PVT thermal energy for possible reuse after sunset. The concept of sustainability should be extended in the PVT studies along with the economic and environmental approaches to view a wider indication of this technology.

Table 4
Summary of main outcomes of previous studies compared with the current study findings.

Reference	Nanofluid type	Concentration	PVT efficiency advancements		
			Thermal efficiency	Electric efficiency	Exergy efficiency
Khanjari et al. [77]	Ag	0.05 %	84.8 %	11.4 %	15.4 %
	Al_2O_3		82 %	11.2 %	15 %
Alktranee et al. [79]	CuO	0.2 %	36.7 %	9.2 %	9.7 %
		0.3 %	38.9 %	10.3 %	10.91 %
	Fe_2O_3	0.2 %	40.8 %	11.3 %	12.22 %
		0.3 %	43.3 %	12.1 %	13.01 %
Sardarabadi et al. [81]	TiO_2	0.2 %	44.34 %	13.63 %	11.93 %
	ZnO		46.05 %	13.59 %	12.17 %
	Al_2O_3		36.66 %	13.44 %	11.88 %
Hosseinzadeh et al. [82]	ZnO	12 %	55.3 %	14.24 %	–
Fayaz et al. [83]	MWCNT	0.75 %	79.1 %	12.37 %	–
			81.24 %	12.5 %	
AL-Musawi et al. [84]	SiO_2	1 %	36 %	30 %	–
		3 %	40 %	31 %	
Current study	Fe_2O_3	0.2 %	29.89 %	11.15 %	11.15 %
		0.3 %	32.79 %	11.8 %	12.21 %
	TiO_2- Fe_2O_3	0.2 %	41.48 %	12.74 %	14.11 %
		0.3 %	43.5 %	12.93 %	15.11 %

CRediT authorship contribution statement

Mohammed Alktranee: Writing – original draft, Validation, Software, Methodology, Investigation, Formal analysis, Conceptualization. **Qudama Al-Yasiri:** Writing – original draft, Validation, Investigation, Formal analysis. **Karrar Saeed Mohammed:** Writing – review & editing, Methodology, Formal analysis. **Hayder Al-Lami:** Writing – review & editing, Investigation, Formal analysis. **Péter Bencs:** Writing – review & editing, Supervision, Funding acquisition, Conceptualization.

Declaration of competing interest

The authors declare that they have no known competing financial interests or personal relationships that could have appeared to influence the work reported in this paper.

Acknowledgements

This research was supported by the University of Miskolc and by the agreement between the Hungarian consortium EISZ and Elsevier.

Data availability

Data will be made available on request.

References

[1] Dorian JP, Franssen HT, Simbeck DR. Global challenges in energy. Energy Policy 2006;34:1984–91. https://doi.org/10.1016/j.enpol.2005.03.010.
[2] Das D, Kalita P, Roy O. Flat plate hybrid photovoltaic-thermal (PV/T) system: A review on design and development. Renew Sustain Energy Rev 2018;84:111–30. https://doi.org/10.1016/j.rser.2018.01.002.
[3] Ahmadizadeh M, Heidari M, Thangavel S, Al Naamani E, Khashehchi M, Verma V, et al. Technological advancements in sustainable and renewable solar energy systems. Highly Effic. Therm. Renew. Energy Syst., CRC Press; 2024, p. 23–39.
[4] Alaaeddin MH, Sapuan SM, Zuhri MYM, Zainudin ES, AL-Oqla FM. Photovoltaic applications: Status and manufacturing prospects. Renew Sustain Energy Rev 2019; 102:318–32. https://doi.org/10.1016/j.rser.2018.12.026.
[5] Predicting Solar Power Generation Utilized in Iraq Power Grid Using Neural Network. Misan J Eng Sci 2024;3:38–62. 10.61263/mjes.v3i1.72.
[6] Sarbu I, Sebarchievici C. Review of solar refrigeration and cooling systems. Energy Build 2013;67:286–97. https://doi.org/10.1016/j.enbuild.2013.08.022.
[7] Ogbomo OO, Amalu EH, Ekere NN, Olagbegi PO. A review of photovoltaic module technologies for increased performance in tropical climate. Renew Sustain Energy Rev 2017;75:1225–38. https://doi.org/10.1016/j.rser.2016.11.109.
[8] Luo W, Khoo YS, Hacke P, Naumann V, Lausch D, Harvey SP, et al. Potential-induced degradation in photovoltaic modules: a critical review. Energy Environ Sci 2017;10:43–68. https://doi.org/10.1039/C6EE02271E.
[9] Hasan HA, Ajeel KI. Preparation of Poly O-Toluidine/Titanium Dioxide by In situ Chemical Oxidation Polymerization and Application for Solar Cell. J Misan Res 2020;16:382–400. https://doi.org/10.52834/jmr.v16i31.35.
[10] Dwivedi P, Sudhakar K, Soni A, Solomin E, Kirpichnikova I. Advanced cooling techniques of P.V. modules: A state of art. Case Stud. Therm Eng 2020;21:100674. https://doi.org/10.1016/j.csite.2020.100674.
[11] Mahdavi A, Farhadi M, Gorji-Bandpy M, Mahmoudi A. A comprehensive study on passive cooling of a PV device using PCM and various fin configurations: Pin, spring, and Y-shaped fins. Appl Therm Eng 2024;252:123519. https://doi.org/10.1016/j.applthermaleng.2024.123519.
[12] Bashtani I, Esfahani JA. Improving the photovoltaic thermal system efficiency with nature-inspired dolphin turbulators from energy and exergy viewpoints. Renew Energy 2024;231:120931. https://doi.org/10.1016/j.renene.2024.120931.
[13] Al-Lami H, Al-Mayyahi NN, Al-Yasiri Q, Ali R, Alshara A. Performance enhancement of photovoltaic module using finned phase change material panel: An experimental study under Iraq hot climate conditions. Energy Sources, Part A Recover Util Environ Eff 2022;44:6886–97. https://doi.org/10.1080/15567036.2022.2103601.
[14] Vaziri Rad MA, Rousta M, Khanalizadeh A, Kouravand A, Akbari M, Mousavi S, et al. Critical analysis of enhanced photovoltaic thermal systems: a comparative experimental study of PCM, TEG, and nanofluid applications. Energy Convers Manag 2024;314:118712. https://doi.org/10.1016/j.enconman.2024.118712.
[15] Alshammari AA, Salilih EM, Almatrafi E, Rady M. Polymeric coatings for passive radiative cooling of PV modules in hot and humid weather: Design, optimization, and performance evaluation. Case Stud Therm Eng 2024;57:104341. https://doi.org/10.1016/j.csite.2024.104341.
[16] Azam MS, Bhattacharjee A, Hassan M, Rahaman M, Aziz S, Ali Shaikh MA, et al. Performance enhancement of solar PV system introducing semi-continuous tracking algorithm based solar tracker. Energy 2024;289:129989. https://doi.org/10.1016/j.energy.2023.129989.
[17] Farahani SD, Zare MK, Alizadeh A. Enhancing PVT/air system performance with impinging jet and porous media: A computational approach with machine learning predictions. Appl Energy 2025;377:124509. https://doi.org/10.1016/j.apenergy.2024.124509.
[18] Salman AHA, Hilal KH, Ghadhban SA. Enhancing performance of PV module using water flow through porous media. Case Stud Therm Eng 2022;34:102000. https://doi.org/10.1016/j.csite.2022.102000.
[19] Ul-Abdin Z, Zeman M, Isabella O, Santbergen R. Investigating the annual performance of air-based collectors and novel bi-fluid based PV-thermal system. Sol Energy 2024;276:112687. https://doi.org/10.1016/j.solener.2024.112687.
[20] Jafari R. Optimization and energy analysis of a novel geothermal heat exchanger for photovoltaic panel cooling. Sol Energy 2021;226:122–33. https://doi.org/10.1016/j.solener.2021.08.046.
[21] Madhi H, Aljabair S, Imran AA. A review of photovoltaic/thermal system cooled using mono and hybrid nanofluids. Int J Thermofluids 2024;22:100679. https://doi.org/10.1016/j.ijft.2024.100679.
[22] Abd-Elhady MM, Elhendawy MA, Abd-Elmajeed MS, Rizk RB. Enhancing photovoltaic systems: A comprehensive review of cooling, concentration, spectral splitting, and tracking techniques. Next Energy 2025;6:100185. https://doi.org/10.1016/j.nxener.2024.100185.
[23] Rajaee F, Rad MAV, Kasaeian A, Mahian O, Yan W-M. Experimental analysis of a photovoltaic/thermoelectric generator using cobalt oxide nanofluid and phase change material heat sink. Energy Convers Manag 2020;212:112780. https://doi.org/10.1016/j.enconman.2020.112780.
[24] Saeed S, Hussain A, Ali I, Shahid H, Anwar M, Ali HM. Photovoltaic Module Efficiency Enhancement System by Novel Cooling Techniques: Effect of Phase Change Material and Fins. Process Saf Environ Prot 2024. https://doi.org/10.1016/j.psep.2024.06.105.
[25] Akrouch MA, Chahine K, Faraj J, Hachem F, Castelain C, Khaled M. Advancements in cooling techniques for enhanced efficiency of solar photovoltaic panels: A detailed comprehensive review and innovative classification. Energy Built Environ 2023. https://doi.org/10.1016/j.enbenv.2023.11.002.
[26] Ibrahim OAAM, Kadhim SA, Al-Ghezi MKS. Photovoltaic panels cooling technologies: Comprehensive review. Arch Thermodyn 2023;44:581–617. https://doi.org/10.24425/ather.2023.149720.
[27] Dunne NA, Liu P, Elbarghthi AFA, Yang Y, Dvorak V, Wen C. Performance evaluation of a solar photovoltaic-thermal (PV/T) air collector system. Energy Convers Manag X 2023;20:100466. https://doi.org/10.1016/j.ecmx.2023.100466.
[28] Pang W, Zhang Y, Duck BC, Yu H, Song X, Yan H. Cross sectional geometries effect on the energy efficiency of a photovoltaic thermal module: Numerical simulation and experimental validation. Energy 2020;209:118439. https://doi.org/10.1016/j.energy.2020.118439.
[29] Ho CJ, Peng J-K, Yang T-F, Rashidi S, Yan W-M. Comparison of cooling performance of nanofluid flows in mini/micro-channel stacked double-layer heat sink and single-layer micro-channel heat sink. Int J Therm Sci 2023;191:108375. https://doi.org/10.1016/j.ijthermalsci.2023.108375.
[30] Ho CJ, Peng JK, Yang TF, Rashidi S, Yan WM. On the assessment of the thermal performance of microchannel heat sink with nanofluid. Int J Heat Mass Transf 2023;201:123572. https://doi.org/10.1016/j.ijheatmasstransfer.2022.123572.
[31] Parthiban A, Reddy KS, Pesala B, Mallick TK. Effects of operational and environmental parameters on the performance of a solar photovoltaic-thermal collector. Energy Convers Manag 2020;205:112428. https://doi.org/10.1016/j.enconman.2019.112428.
[32] Aberoumand S, Ghamari S, Shabani B. Energy and exergy analysis of a photovoltaic thermal (PV/T) system using nanofluids: An experimental study. Sol Energy 2018; 165:167–77. https://doi.org/10.1016/j.solener.2018.03.028.
[33] Le Ba T, Baqer A, Saad Kamel M, Gróf G, Odhiambo VO, Wongwises S, et al. Experimental Study of Halloysite Nanofluids in Pool Boiling Heat Transfer. Molecules 2022;27:729. https://doi.org/10.3390/molecules27030729.
[34] Tawalbeh M, Shomope I, Al-Othman A. Comprehensive review on non-Newtonian nanofluids, preparation, characterization, and applications. Int J Thermofluids 2024;22:100705. https://doi.org/10.1016/j.ijft.2024.100705.
[35] Olabi AG, Elsaid K, Sayed ET, Mahmoud MS, Wilberforce T, Hassiba RJ, et al. Application of nanofluids for enhanced waste heat recovery: A review. Nano Energy 2021;84:105871. https://doi.org/10.1016/j.nanoen.2021.105871.
[36] Shah TR, Ali HM. Applications of hybrid nanofluids in solar energy, practical limitations and challenges: A critical review. Sol Energy 2019;183:173–203. https://doi.org/10.1016/j.solener.2019.03.012.
[37] Aljibory MS, Alsulayfani PDBJ, Mahmood PDMN. Improvement of Concrete Mechanical Properties by Adding Nanomaterials. Misan J Eng Sci 2023;2:57–70. 10.61263/mjes.v2i2.62.
[38] Daraee M, Hassani SS, Saeedirad R. Chapter 21 - Nanomaterials in the transportation industry. In: Malik MI, Hussain D, Shah MR, Guo D-S, editors. Handb. Nanomater. Vol. 1, Elsevier; 2024, p. 567–91. 10.1016/B978-0-323-95511-9.00018-4.
[39] Sharaby MR, Younes M, Baz F, Abou-Taleb F. State-of-the-Art Review: Nanofluids for Photovoltaic Thermal Systems. J Contemp Technol Appl Eng 2024;3:11–24. https://doi.org/10.21608/jctae.2024.288445.1025.
[40] Farag MM, Hamid A-K, AlMallahi MN, Elgendi M. Towards highly efficient solar photovoltaic thermal cooling by waste heat utilization: A review. Energy Convers Manag X 2024;23:100671. https://doi.org/10.1016/j.ecmx.2024.100671.
[41] Chen J, Huang Y, Wang L. Numerical investigation of photovoltaic performance improvement using Al2O3 nanofluid. Chem Eng Res Des 2024. https://doi.org/10.1016/j.cherd.2024.09.011.
[42] Venkatesh T, Manikandan S, Selvam C, Harish S. Performance enhancement of hybrid solar PV/T system with graphene based nanofluids. Int Commun Heat Mass

Transf 2022;130:105794. https://doi.org/10.1016/j.icheatmasstransfer.2021.105794.
[43] Menon GS, Murali S, Elias J, Aniesrani Delfiya DS, Alfiya PV, Samuel MP. Experimental investigations on unglazed photovoltaic-thermal (PVT) system using water and nanofluid cooling medium. Renew Energy 2022;188:986–96. https://doi.org/10.1016/j.renene.2022.02.080.
[44] Nasrin R, Rahim NA, Fayaz H, Hasanuzzaman M. Water/MWCNT nanofluid based cooling system of PVT: Experimental and numerical research. Renew Energy 2018;121:286–300. https://doi.org/10.1016/j.renene.2018.01.014.
[45] Hissouf M, Najim M, Charef A. Numerical study of a covered Photovoltaic-Thermal Collector (PVT) enhancement using nanofluids. Sol Energy 2020;199:115–27.
[46] Fudholi A, Razali NFM, Yazdi MH, Ibrahim A, Ruslan MH, Othman MY, et al. TiO2/water-based photovoltaic thermal (PVT) collector: Novel theoretical approach. Energy 2019;183:305–14. https://doi.org/10.1016/j.energy.2019.06.143.
[47] Sardarabadi M, Passandideh-Fard M. Experimental and numerical study of metal-oxides/water nanofluids as coolant in photovoltaic thermal systems (PVT). Sol Energy Mater Sol Cells 2016;157:533–42.
[48] Dashtbozorg A, Rohani R, Jahanshahi R, Shanbedi M, Akbarzadeh E, Hatamifar B. Investigating the effect of MXene/ethanol nanofluid in thermosyphon cooling of hybrid photovoltaic/thermal (PV/T) panels. Int J Heat Fluid Flow 2024;107:109389. https://doi.org/10.1016/j.ijheatfluidflow.2024.109389.
[49] Shaik AH, Chakraborty S, Saboor S, Kumar KR, Majumdar A, Rizwan M, et al. Cu-Graphene water-based hybrid nanofluids: synthesis, stability, thermophysical characterization, and figure of merit analysis. J Therm Anal Calorim 2024;149:2953–68. https://doi.org/10.1007/s10973-023-12875-x.
[50] Sharaby MR, Younes MM, Abou-Taleb FS, Baz FB. The influence of using MWCNT/ZnO-Water hybrid nanofluid on the thermal and electrical performance of a Photovoltaic/Thermal system. Appl Therm Eng 2024;248:123332. https://doi.org/10.1016/j.applthermaleng.2024.123332.
[51] Kazemian A, Salari A, Ma T, Lu H. Application of hybrid nanofluids in a novel combined photovoltaic/thermal and solar collector system. Sol Energy 2022;239:102–16.
[52] Hooshmandzade N, Motevali A, Seyedi SRM, Biparva P. Influence of single and hybrid water-based nanofluids on performance of microgrid photovoltaic/thermal system. Appl Energy 2021;304:117769.
[53] Alktranee M, Shehab MA, Németh Z, Bencs P, Hernadi K. Thermodynamic analysis of mono and hybrid nanofluid effect on the photovoltaic-thermal system performance: A comparative study. Heliyon 2023;9.
[54] Muneeshwaran M, Srinivasan G, Muthukumar P, Wang C-C. Role of hybrid-nanofluid in heat transfer enhancement – A review. Int Commun Heat Mass Transf 2021;125:105341. https://doi.org/10.1016/j.icheatmasstransfer.2021.105341.
[55] Alktranee M, Shehab MA, Németh Z, Bencs P, Hernadi K. Experimental study for improving photovoltaic thermal system performance using hybrid titanium oxide-copper oxide nanofluid. Arab J Chem 2023:105102.
[56] Che Sidik NA, Mahmud Jamil M, Aziz Japar WMA, Muhammad AI. A review on preparation methods, stability and applications of hybrid nanofluids. Renew Sustain Energy Rev 2017;80:1112–22. https://doi.org/10.1016/j.rser.2017.05.221.
[57] Pak BCC, Cho YII. Hydrodynamic and heat transfer study of dispersed fluids with submicron metallic oxide particles. Exp Heat Transf 1998;11:151–70. https://doi.org/10.1080/08916159808946559.
[58] Yu W, Choi SUS. The role of interfacial layers in the enhanced thermal conductivity of nanofluids: a renovated Maxwell model. J Nanoparticle Res 2003;5:167–71.
[59] Xuan Y, Roetzel W. Conceptions for heat transfer correlation of nanofluids. Int J Heat Mass Transf 2000;43:3701–7. https://doi.org/10.1016/S0017-9310(99)00369-5.
[60] Brinkman HC. The viscosity of concentrated suspensions and solutions. J Chem Phys 1952;20:571.
[61] Abbas F, Ali HM, Shaban M, Janjua MM, Shah TR, Doranehgard MH, et al. Towards convective heat transfer optimization in aluminum tube automotive radiators: Potential assessment of novel Fe2O3-TiO2/water hybrid nanofluid. J Taiwan Inst Chem Eng 2021;124:424–36.
[62] Namjoo A, Sarhaddi F, Sobhnamayan F, Alavi MA, Mahdavi Adeli M, Farahat S. Exergy performance analysis of solar photovoltaic thermal (PV/T) air collectors in terms of exergy losses. J Energy Inst 2011;84:132–45.
[63] Yu Y, Long E, Chen X, Yang H. Testing and modelling an unglazed photovoltaic thermal collector for application in Sichuan Basin. Appl Energy 2019;242:931–41.
[64] Alktranee M, Bencs P. Applications of nanotechnology with hybrid photovoltaic/thermal systems: A review. J Appl Eng Sci 2021;19:292–306. https://doi.org/10.5937/jaes0-28760.
[65] Rukman NSB, Fudholi A, Razali NFM, Ruslan MH, Sopian K. Energy and exergy analyses of photovoltaic-thermal (PV/T) system with TiO2/water nanofluid flow. IOP Conf. Ser. Earth Environ. Sci., vol. 268, IOP Publishing; 2019, p. 12075.
[66] Al-Waeli AHA, Chaichan MT, Kazem HA, Sopian K, Safaei J. Numerical study on the effect of operating nanofluids of photovoltaic thermal system (PV/T) on the convective heat transfer. Case Stud Therm Eng 2018;12:405–13.
[67] Hussein AM, Bakar RA, Kadirgama K, Sharma KV. Experimental measurement of nanofluids thermal properties. Int J Automot Mech Eng 2013;7:850.
[68] Qiu Z, Zhao X, Li P, Zhang X, Ali S, Tan J. Theoretical investigation of the energy performance of a novel MPCM (Microencapsulated Phase Change Material) slurry based PV/T module. Energy 2015;87:686–98.
[69] Jha P, Mondol JD, Das B, Gupta R. Energy metrics assessment of a photovoltaic thermal air collector (PVTAC): a comparison between flat and wavy collector. Energy Sources, Part A Recover Util Environ Eff 2020:1–19.
[70] Alomar OR, Ali OM. Energy and exergy analysis of hybrid photovoltaic thermal solar system under climatic condition of North Iraq. Case Stud Therm Eng 2021;28:101429. https://doi.org/10.1016/j.csite.2021.101429.
[71] Fudholi A, Zohri M, Jin GL, Ibrahim A, Yen CH, Othman MY, et al. Energy and exergy analyses of photovoltaic thermal collector with∇-groove. Sol Energy 2018;159:742–50.
[72] Maadi SR, Kolahan A, Passandideh-Fard M, Sardarabadi M, Moloudi R. Characterization of PVT systems equipped with nanofluids-based collector from entropy generation. Energy Convers Manag 2017;150:515–31.
[73] Corbin CD, Zhai ZJ. Experimental and numerical investigation on thermal and electrical performance of a building integrated photovoltaic–thermal collector system. Energy Build 2010;42:76–82.
[74] Mahmoudi AH, Shahi M, Shahedin AM, Hemati N. Numerical modeling of natural convection in an open cavity with two vertical thin heat sources subjected to a nanofluid. Int Commun Heat Mass Transf 2011;38:110–8.
[75] Lin KC, Violi A. Natural convection heat transfer of nanofluids in a vertical cavity: Effects of non-uniform particle diameter and temperature on thermal conductivity. Int J Heat Fluid Flow 2010;31:236–45.
[76] Demir H, Dalkilic AS, Kürekci NA, Duangthongsuk W, Wongwises S. Numerical investigation on the single phase forced convection heat transfer characteristics of TiO2 nanofluids in a double-tube counter flow heat exchanger. Int Commun Heat Mass Transf 2011;38:218–28.
[77] Khanjari Y, Pourfayaz F, Kasaeian AB. Numerical investigation on using of nanofluid in a water-cooled photovoltaic thermal system. Energy Convers Manag 2016;122:263–78.
[78] Khelifa A, Touafek K, Ben Moussa H, Tabet I. Modeling and detailed study of hybrid photovoltaic thermal (PV/T) solar collector. Sol Energy 2016;135:169–76. https://doi.org/10.1016/j.solener.2016.05.048.
[79] Alktranee M, Al-Yasiri Q, Shehab MA, Bencs P, Németh Z, Hernadi K. Experimental and numerical study of a photovoltaic/thermal system cooled by metal oxide nanofluids. Alexandria Eng J 2024;94:55–67.
[80] Awais M, Ullah N, Ahmad J, Sikandar F, Ehsan MM, Salehin S, et al. Heat transfer and pressure drop performance of Nanofluid: A state-of- the-art review. Int J Thermofluids 2021;9:100065. https://doi.org/10.1016/j.ijft.2021.100065.
[81] Sardarabadi M, Hosseinzadeh M, Kazemian A, Passandideh-Fard M. Experimental investigation of the effects of using metal-oxides/water nanofluids on a photovoltaic thermal system (PVT) from energy and exergy viewpoints. Energy 2017;138:682–95. https://doi.org/10.1016/j.energy.2017.07.046.
[82] Hosseinzadeh M, Salari A, Sardarabadi M, Passandideh-Fard M. Optimization and parametric analysis of a nanofluid based photovoltaic thermal system: 3D numerical model with experimental validation. Energy Convers Manag 2018;160:93–108. https://doi.org/10.1016/j.enconman.2018.01.006.
[83] Fayaz H, Nasrin R, Rahim NA, Hasanuzzaman M. Energy and exergy analysis of the PVT system: Effect of nanofluid flow rate. Sol Energy 2018;169:217–30. https://doi.org/10.1016/j.solener.2018.05.004.
[84] AL-Musawi AIA, Taheri A, Farzanehnia A, Sardarabadi M, Passandideh-Fard M. Numerical study of the effects of nanofluids and phase-change materials in photovoltaic thermal (PVT) systems. J Therm Anal Calorim 2019;137:623–36. https://doi.org/10.1007/s10973-018-7972-6.